

## ON THE NONLINEAR MODELING OF PARAMETRIC ROLLING IN REGULAR AND IRREGULAR WAVES

Gabriele Bulian, Alberto Francescutto, DINMA, University of Trieste, (Italy)  
Claudio Lugni, INSEAN, (Italy)

### Abstract

This paper summarizes the results and the problems still open regarding the development of a 1.5DOF nonlinear mathematical model of the parametric rolling in longitudinal waves with particular regard to the head sea condition. A first part is devoted to the case of regular waves, while the second concerns parametric rolling generated by irregular waves obtained by means of white noise filtered through a linear filter with adjustable bandwidth and by using a Bretschneider spectrum. The availability of an extensive series of test results on scale models conducted at University of Trieste and at INSEAN, allows a thorough discussion of the problems connected with the threshold formulation for parametric rolling and its amplitude modelling above threshold.

### 1 INTRODUCTION

The aim of this paper is that of developing a simplified mathematical model for the prediction of the excitation threshold and of the amplitude above threshold of parametric rolling. In this context simplified means using a low number of degrees of freedom in order have the possibility of obtaining an approximate solution in analytical form, preserving on the other hand the fully nonlinear and stochastic features of the phenomenon. To this end, a large series of tests have been started at the University of Trieste and at INSEAN on the scale model of a RoRo. The threshold of the first and second parametric resonance have been investigated in regular waves, while the irregular wave tests, focussed for the moment on the analysis of the first zone, investigated in some detail the effect of the shape and bandwidth of the spectrum. The capability and limits of two nonlinear stochastic approximate solutions of the

mathematical model are also discussed in the paper.

### 2 PARAMETRIC ROLL IN REGULAR WAVES

#### 2.1 Analytical model

A ship sailing in a longitudinal sea in upright position is subjected to the action of symmetrical motions and waves. Regarding the problem of parametric rolling, three phenomena should be taken into consideration:

- heave motion
- pitch motion
- wave effect

The combined action of wave and vertical motions leads to a fluctuation (in time) of the restoring characteristics of the ship.

Because the large amplitude motions we are dealing with when we are addressing the problem of parametric roll, all six degrees of

freedom should be considered as coupled. On the other hand, for the particular case reported in this paper, the experiments have been performed with the model fairly restrained in surge, yaw and sway, whereas pitch, heave and roll were almost completely free. The sea was, moreover, longitudinal and long crested.

The analysis could thus take into consideration only the three free degrees of freedom. The influence of roll on pitch and heave could be modelled as an explicit forcing (with frequency equal to twice the roll frequency, thus equal to the encounter frequency due to the subharmonic regime of the response), whereas the influence of heave and pitch on roll can be modelled as a parametric excitation.

The wave induces heave and pitch, modifies the hull geometry and the pressure field around the hull.

If the displacement of the ship can be considered as constant, the roll motion equation can be written in the following form:

$$\ddot{\phi} + d(\phi, \dot{\phi}) + \omega_0^2 \cdot \frac{\overline{GZ}(\phi, \vartheta, \eta, \xi_c)}{GM} = 0 \quad (1)$$

where  $\vartheta$  is the pitch angle,  $\eta$  the heave displacement and  $\xi_c$  the wave crest position along the ship.

If, moreover, we are able to correlate  $\vartheta$  and  $\eta$  with  $\xi_c$  and  $\phi$ , that is

$$\begin{cases} \vartheta = \vartheta(\xi_c, \phi) \\ \eta = \eta(\xi_c, \phi) \end{cases} \quad (2)$$

the restoring term becomes

$$\overline{GZ}(\phi, \xi_c) = \overline{GZ}(\phi, t) \quad (3)$$

and the explicit dependence on time can be obtained when the ship speed, the wave celerity and the encounter angle are known.

Finally, the equation of motion for the 1.5-DOF roll motion becomes:

$$\ddot{\phi} + d(\phi, \dot{\phi}) + \omega_0^2 \cdot \frac{\overline{GZ}(\phi, t)}{GM} = 0 \quad (4)$$

When we are dealing with regular waves, the function  $\overline{GZ}(\phi, t)$  is periodic with period  $T_e$  equal to the encounter period between ship and wave.

A first attempt to analyse the equation (4) is based on the analysis of the fluctuation of the righting arm around the still water (SW) value. Let

$$\overline{GZ}(\phi, t) = \overline{GZ}_{SW}(\phi) + \delta\overline{GZ}(\phi, t) \quad (5)$$

where  $\delta\overline{GZ}(\phi, t)$  represents the variation of the righting arm respect to the still water condition. An example of the calculated variation is reported for the model TR2 in Fig. 1. The characteristics and the body plan of the model TR2 used in the experiments are reported in Table 1.

Table 1: Body plan, model and full scale data of RoRo pax TR2 used in the experiments.

<b>RoRo pax TR2 - C73-97</b>
<b>Full scale data:</b>
$\Delta=7715 \text{ t}_f$
$GM=0.865 \text{ m}$
$KG=8.660 \text{ m}$
$T=5.875 \text{ m}$
$x_G=-3.599 \text{ m}$
$L_{bp}=132.2 \text{ m}$
$T_0=16.26 \text{ s}$
<b>Scale of tested model 1:50</b>

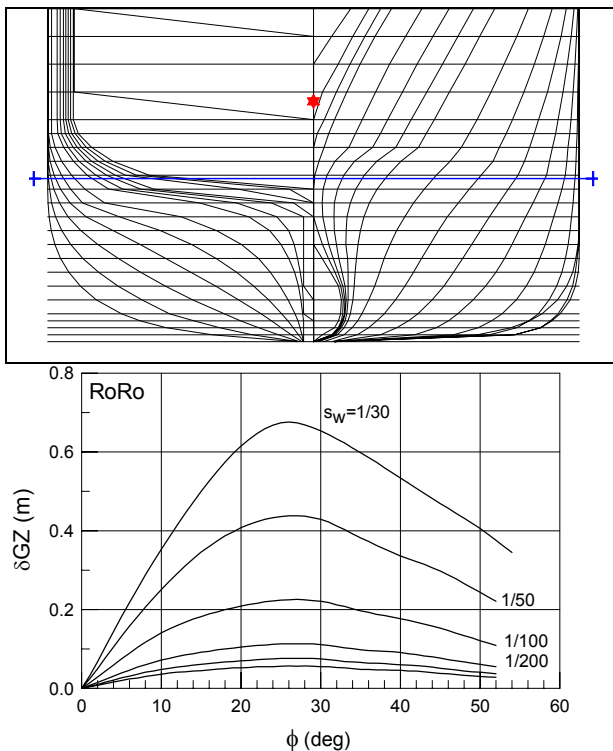


Fig. 1: Difference between the righting arm corresponding to wave through amidships and wave crest amidships as a function of the transversal inclination. The curves refer to wave steepness  $sw=1/30, 1/50, 1/100, 1/200, 1/300$ .

As explained in [6] and [2], under some approximations, we can write

$$\begin{aligned} \overline{GZ}(\phi, t) &= \\ &= \overline{GM} \cdot \phi \cdot (1 + h_0(\phi) \cdot \cos(\omega_e \cdot t + \psi)) + K_3 \cdot \phi^3 \end{aligned} \quad (6)$$

being

$$h_0(\phi) = p_1 + p_2 \cdot \phi^2 \quad (7)$$

With an appropriate time translation and using a linear plus cubic model for the damping term the roll equation becomes

$$\begin{aligned} \ddot{\phi} + 2\mu\dot{\phi} + \delta \cdot \phi^3 + \\ + \omega_0^2 \phi \cdot [1 + (p_1 + p_2 \phi^2) \cos \omega_e t] + \alpha_3 \phi^3 = 0 \end{aligned} \quad (8)$$

This equation represents the so called "uncoupled" model as reported in [6]. The parameter  $\alpha_3$  should be considered as a constant and should be obtained from the analysis of the still water righting arm. The parameter  $p_1$  represents the relative variation of the metacentric height, whereas the parameter  $p_2$  is used in order to take into consideration some nonlinear aspects of the righting arm fluctuation (see Fig. 1). The values of the parameters  $p_1$  and  $p_2$  depends on the wave height, the wave length and the assumptions done about the relation between heave, pitch and wave position. Basically three approaches can be used [6]:

- fix trim hydrostatic
- free trim hydrostatic
- dynamic (based on seakeeping calculation)

The chosen approach modifies both the still water righting arm and the righting arm on wave. Only when the third approach is used (dynamic) a variation of the displacement in time must be taken into consideration.

Using a direct analysis of the righting arm in waves as proposed in [2] (that is without splitting  $\overline{GZ}$  in a still water part and a wave fluctuation component) the problem of calculating  $\overline{GZ}_{SW}$  would be avoided.

The linearised version of the model represented by equation (8) is a Mathieu equation that is known [6],[11],[20] to exhibit instability of the solution  $\phi=0$  when the ratio between encounter frequency and natural frequency is in the range

$$\frac{\omega_e}{\omega_0} \approx \frac{2}{n} \quad n=1,2,3,\dots \quad (9)$$

as one can see from Fig. 2 [7]. The dashed zones represent regions of parameter space

where the Mathieu equation shows instability of the trivial solution.

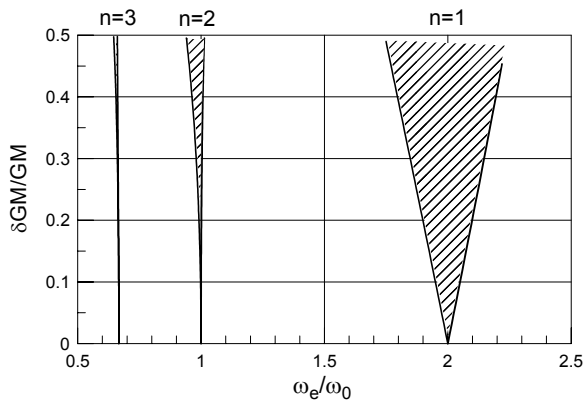


Fig. 2: Threshold boundaries of the first three instability zones for the linear undamped Mathieu equation. The diagram has been adapted to variables relevant to parametric rolling.

The presence of damping changes quantitatively the picture giving a minimum value for the threshold in proximity of the exact synchronism. This minimum value of the instability threshold depends on the linear damping and on the zone index as follows:

$$p_1 \propto \left( \frac{\mu}{\omega_0} \right)^{\frac{1}{n}} \tag{10}$$

Linking the analytical results known for the Mathieu equation and the calculation of the parametric excitation by means of a standard hydrostatic software, the instability boundaries can be predicted [6] as reported in Fig. 3 .

The linearised equation predicts a growing without bounds of the solution in the instability region. When a nonlinear model (in restoring and/or damping) is used, the possibility of bounded solution is predicted. Damping nonlinearities tend to reduce the motion because of the larger energy dissipation rate at larger amplitude of motion, whereas restoring nonlinearities reduce motion amplitude due to the detuning effect. As reported in past papers [9] the effect of nonlinear damping seems to be

of less importance when compared with the effect of the nonlinear restoring.

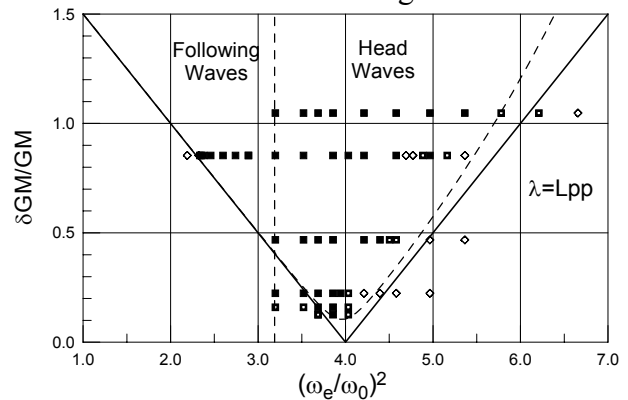


Fig. 3: Comparison between experimental results and analytical threshold curves. The stability calculations were made with fixed trim.

The model proposed in equation (8) can be tackled using approximate analytical techniques such as the averaging method [7] and the amplitude of motion above threshold can be expressed as a function of the parameters.

The behaviour of the experimental results obtained at the DINMA towing tanks in the case of wave steepness equal to 1/50 and different wave length is reported in Fig. 4.

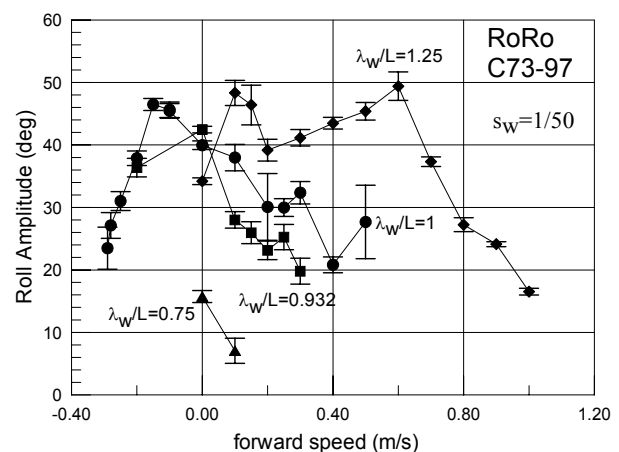


Fig. 4: Steady roll motion amplitude of parametric rolling as a function of ship forward speed (given at model scale) at constant wave steepness.

A fitting of the steady state amplitude of motion above threshold using the model (8) in the case of wave steepness 1/30 and 1/50 is shown in Fig. 5 and Fig. 6.

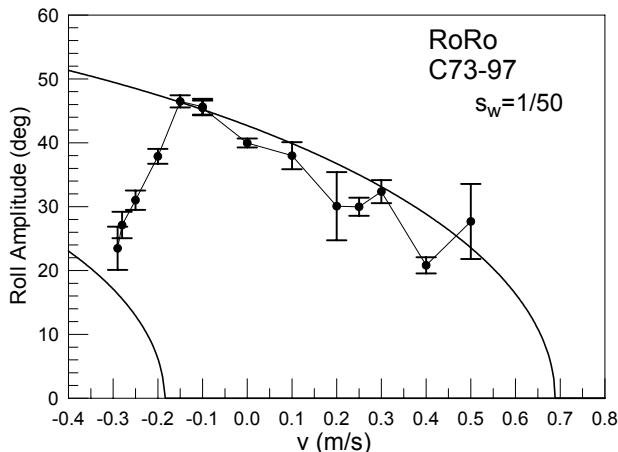


Fig. 5: Steady roll motion amplitude of parametric rolling as a function of ship forward speed (at model scale).  $\lambda_w/L = 1$  and  $s_w = 1/30$ .

As one can see, the behaviour observed from the experiments can be reproduced quite well using the proposed model in equation (8) when parameters are obtained by means of a parameter identification technique [6]. The main characteristics of the phenomenon (presence of bifurcations at low and high speed and large but limited amplitude of motion inside the instability region) are well reproduced. The values of the damping parameters have been obtained from free decay experiments [6].

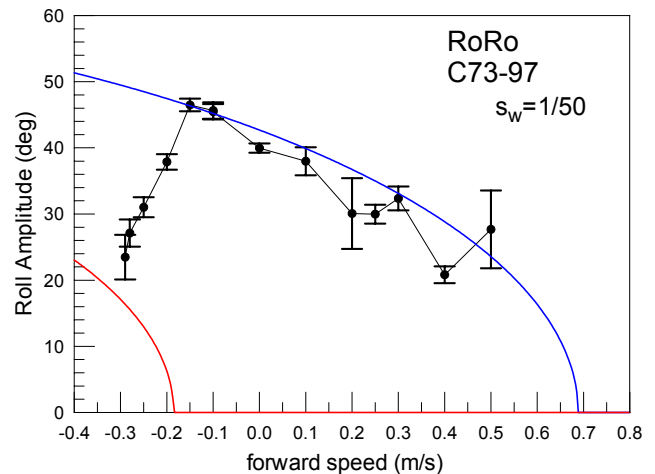


Fig. 6: Steady roll motion amplitude of parametric rolling as a function of ship forward speed (at model scale).  $\lambda_w/L = 1$  and  $s_w = 1/50$ .

In Fig. 6 a smooth decrease of the steady state amplitude of motion can be seen in following sea. The proposed model (8) is not able to reproduce this behaviour, probably due to the fact that only a little part of nonlinear contribution arising from the fluctuation of the restoring lever has been taken into consideration.

## 2.2 Numerical model

In order to evaluate the influence of the whole  $\overline{GZ}$  fluctuation, a fully numerical approach (regarding the restoring term) in time domain has been undertaken. The equation (4) has been used for describing the motion with a linear plus cubic damping model whose coefficients have been obtained from sailing experiments. As a first approach, in this work, the damping coefficients and the natural frequency have been considered as not speed dependent. The mean values in the range of the tested speeds have been used.

The Foude-Krylov hypothesis has been assumed. This assumption is supported by the work of Bogdanov et al. [1]. The procedure is based on an estimation of the value of

$\overline{GZ}(\phi, \xi_C)$  for twenty-one position of the wave crest along ship. A table containing the value of  $\overline{GZ}$  for different heeling angles and different wave crest position is thus created. The motion equation is integrated by means of a Runge-Kutta algorithm and, at each time step, the position of the crest along ship is evaluated (ship speed and wave length are known). When the instantaneous heeling angle is known, and thus the value of  $\overline{GZ}(\phi, \xi_C(t))$  can be evaluated by means of interpolation. When a steady state is achieved, the stationary response is analysed. Two different approaches in the evaluation of  $\overline{GZ}$  have been used:

- free trim hydrostatic
- fix trim hydrostatic

Correction for non-hydrostatic pressure field has been neglected. As reported by Paulling [15], this assumption leads to negligible errors when large heeling angles are considered, whereas it should leads to significant errors in the estimation of the metacentric height fluctuation.

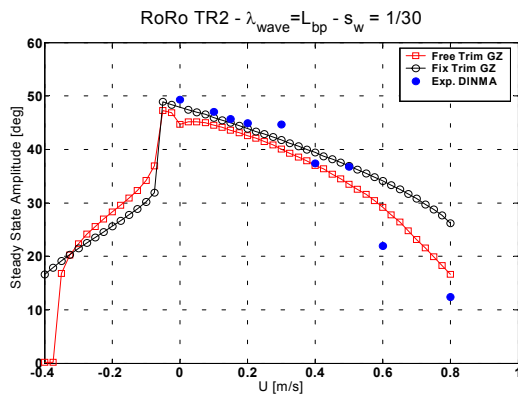


Fig.7: Experimental results and predictions obtained by means of the numerical approach.  $s_W = 1/30$ .

Some comparisons between the experimental results and the prediction obtained by means of the aforementioned procedure are shown in the following figures. For the reported cases the following parameters have been used:

$$\begin{cases} \omega_0 = 2.803 \text{ rad} / \text{s} \\ \delta \cdot \omega_0 = 0.841 \\ \mu / \omega_0 = 0.012 \end{cases}$$

Fig.7 and Fig. 8 report the cases with  $s_W = 1/30$  and  $s_W = 1/50$ .

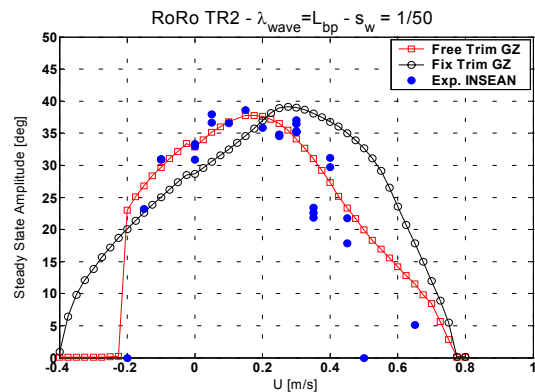


Fig. 8: Experimental results and predictions obtained by means of the numerical approach.  $s_W = 1/50$ .

As one can see from the graphs, the instability zone predicted by the fix trim approach is always larger than that predicted by the free trim approach.

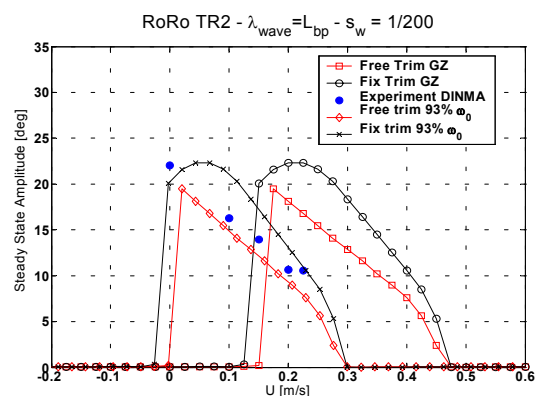


Fig. 9: Experimental results and predictions obtained by means of the numerical approach.  $s_W = 1/200$ .

This is due to the fact that the fluctuations of the righting arm are smaller when  $\overline{GZ}$  is evaluated allowing the trim to vary. This fact leads to an overestimation of the roll amplitude near the limits of the instability zone by the fix trim model. The quite smooth decrease of the

response curve in the low speed and following sea regions is now properly predicted. Looking at the  $s_W = 1/50$  case, the free trim approach seems to give the best agreement with experimental data. The conversely appears for the  $s_W = 1/30$  case. However, in both cases, the maximum amplitude (that could be referred as a design parameter) is quite well predicted by both approaches.

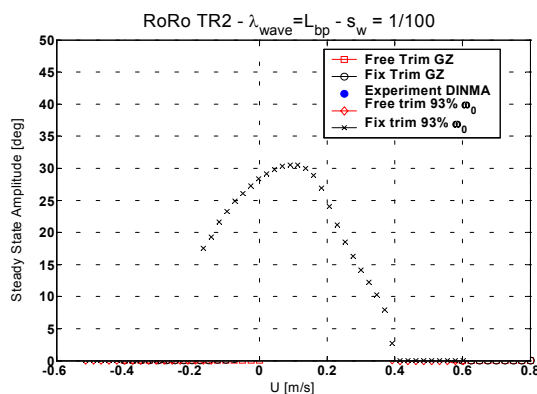


Fig. 10: Experimental results and predictions obtained by means of the numerical approach.  $s_W = 1/100$ .

In the case  $s_W = 1/200$  reported in Fig. 9 a larger disagreement is seen. In order to try to find a better fitting, the roll response predicted by the simulation has been shifted accordingly to a 7% reduction of the natural frequency. This change is equivalent to an increase of the virtual radius of inertia by about 7.5%. Although after this change the agreement between prediction and experimental results looks better, the maximum amplitude is underestimated by the free trim approach, whereas the fix trim approach predicts motion amplitudes close to the maximum experimental value. Unfortunately more experimental points for this particular case would be necessary in order to decide whether or not the prediction is satisfactory. Somewhat similar occurs in the case  $s_W = 1/100$  as can be seen in Fig. 10.

Finally, the agreement between simulation performed using the numerical approach and experiments can be considered quite

satisfactory. From the analysis of the different cases it can't be said which approach (fix trim or free trim) is better. From a conservative point of view, the fix trim approach should be preferred. Moreover the maximum value of the roll amplitude above the instability threshold seems to be predicted quite satisfactory by both approaches, at least in this case, for large values of steepness.

From this numerical simulation, this seems to be a promising simple tool and some work is in progress in order to obtain a "not-too-much-simplified" analytical model based on the analysis of the whole  $\overline{GZ}$  fluctuation.

### 3 PARAMETRIC ROLL IN IRREGULAR SEA

#### 3.1 Introduction to the experiments

The real sea is almost always irregular, thus the parametric excitation induced on the ship roll motion has a stochastic nature.

The general equation (4)

$$\ddot{\phi} + d(\phi, \dot{\phi}) + \omega_0^2 \cdot \frac{\overline{GZ}(\phi, t)}{GM} = 0$$

can be considered still valid, but now  $\overline{GZ}$  is a stochastic process. In a way similar to what has been done in the case of regular sea, two major problems arise when we are dealing with parametric roll in a stochastic environment:

- the determination of the stability threshold
- the evaluation of the statistical properties of the process when stability limits have been exceeded

Regarding the problem of instability threshold, it must be said that many different definition of stochastic stability can be used [2],[8],[12],[13],[16] making the analysis of the stability threshold much more difficult than

that performed when a deterministic excitation is addressed.

A series of experiments have been performed in order to analyse the aforementioned problems. The assumptions of stationarity and ergodicity for the process  $\phi(t)$  have been used in the analysis of the experimental data.

The experiments have been performed at the towing tank of the INSEAN.

Two different sea spectra have been used. The first one is an idealized spectrum obtained by filtering a white noise process with a linear filter [2],[5]:

$$S_z(\omega) = \frac{2 \cdot \gamma \cdot \left( \omega_m^2 + \frac{\gamma^2}{2} \right) \cdot S_0}{\left( \omega_m^2 + \frac{\gamma^2}{2} - \omega^2 \right)^2 + \omega^2 \cdot \gamma^2} \quad (11)$$

The moments of this spectrum have been calculated analytically [2] and thus a simple control of the spectral bandwidth parameter, defined as

$$sbw = \sqrt{\frac{m_0 \cdot m_2}{(m_1)^2} - 1} \quad (12)$$

is possible. When  $sbw$  is close to zero the major part of the energy is concentrated in the vicinity of the modal frequency. The smaller the parameter  $sbw$ , the narrower the band of the process. Moreover  $sbw$  is related to the characteristics of the wave grouping phenomenon [14],[10]. Many tests at different speeds and significant wave heights have been performed using the spectrum (11) with  $sbw$  equal to 0.1,0.25,0.4 in order to analyse the influence of the bandwidth of the sea process on the response.

A Bretschneider spectrum given by the following expression

$$S_z(\omega) = \frac{A}{\omega^5} \cdot \exp\left(-\frac{B}{\omega^4}\right) \quad (13)$$

has been used in order to describe a realistic sea state.

For both spectra the modal wave length has been fixed equal to the  $L_{BP}$ . Different ship speeds in head and following sea have been tested in the vicinity of the condition

$$\omega_{e,m} \approx 2 \cdot \omega_0$$

being  $\omega_{e,m}$  the modal frequency of the sea spectra at the encounter frequencies.

The experimental time series have been analysed and some statistical averages have been calculated, that is:

- roll standard deviation
- roll mean
- roll envelope mean
- roll envelope standard deviation
- significant envelope amplitude (mean of 1/3 of the largest envelope amplitudes)
- maximum roll amplitude

A complete report of the result can be found in [8]. In the following, only the major results are reported.

### 3.2 Experimental results

The experiments have been performed in order to answer to four major questions regarding the problem of parametric rolling in irregular sea. The first question is:

*“Does parametric roll occur in stochastic sea?”*



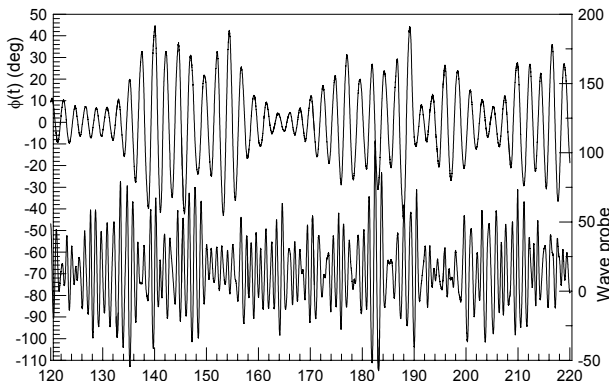


Fig. 11: Comparison between roll (upper) and wave elevation (below) time histories. Bretschneider spectrum,  $V = 0 \text{ m/s}$ ,  $H_{1/3} / L_{BP} = 1/25$ .

Looking at a typical time history reported in Fig. 11 it is possible to say that not only the phenomenon exists, moreover it is, probably, more subtle and dangerous in a stochastic environment than in regular sea. This is due to the fact that, when the parametric excitation is random, the growth of the roll amplitude can be very fast if a sufficiently large group of high waves is encountered by the ship. This can be seen for the case reported in Fig. 11 where, in the initial part of the time history, the amplitude grew from 10deg to almost 50deg in only four roll cycles. Thus the unpredictability (from a deterministic point of view) of the phenomenon and the possible very high rate of growth of the amplitude are the main dangerous characteristics of parametric roll in irregular longitudinal sea.

The second question is:

*“Is the behaviour of the phenomenon similar to what happens in regular sea?”*

In Fig. 12 the roll standard deviation evaluated from the experimental time histories is reported as function of the speed for a Bretschneider sea spectrum with significant wave height equal to 5.3m at full scale. Regarding the other statistical averages, the qualitative behaviour is very similar. A comparison between Fig. 12 and, for example, Fig. 8 shows that the

response in regular sea (presence of an instability zone, bounded amplitude inside the instability region) is qualitatively reproduced by the behaviour in irregular.

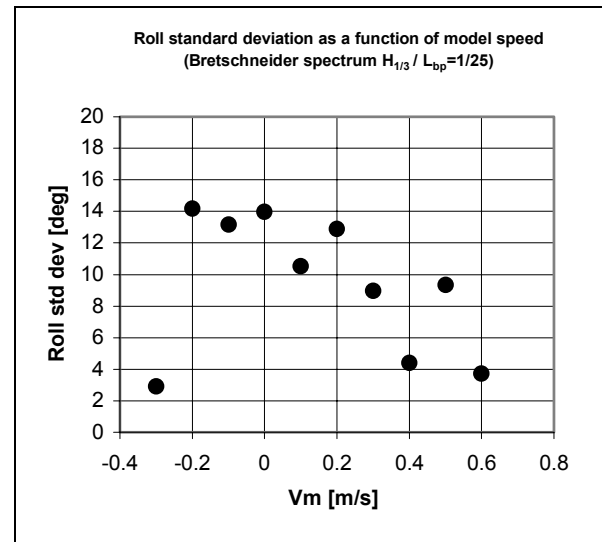


Fig. 12: Estimated experimental roll standard deviation. Bretschneider spectrum,  $H_{1/3} / L_{BP} = 1/25$ .

The third question is:

*“Are the instability regions qualitatively similar to those obtained in regular sea?”*

For the regular sea case, a stability charts has been reported in Fig. 3. The tested cases have been divided is stable, unstable and uncertain conditions after the analysis of the experimental time histories. Deciding whether or not a case should be considered as stable could be a very difficult task, especially when the parametric excitation is not large (as in the case of moderate sea states).

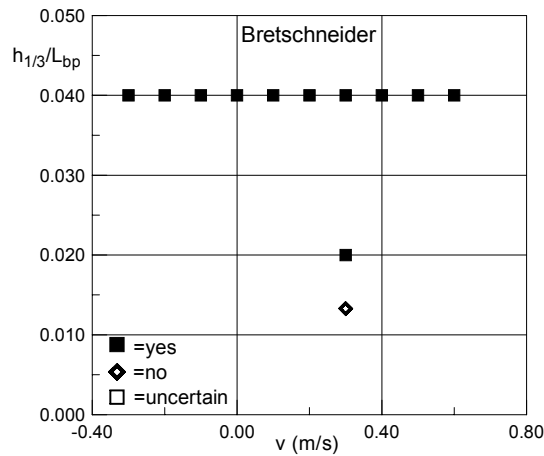


Fig. 13: Stability chart in the case of Bretschneider spectrum.

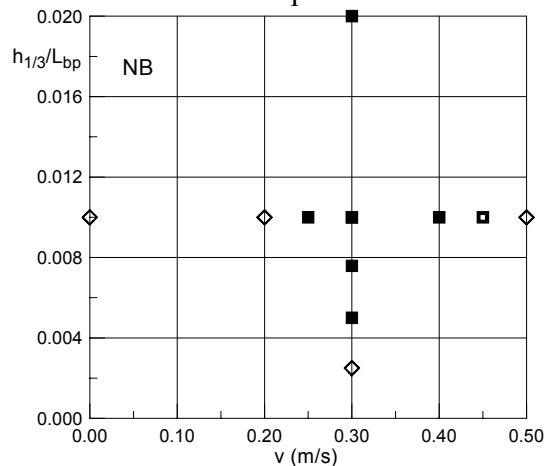


Fig. 14: Stability chart in the case of NB spectrum (theoretical spectrum with  $sbw = 0.1$ ).

From a comparison between Fig. 3, Fig. 13 and Fig. 14 it can be seen that the instability regions in irregular sea have a shape similar to that obtained analytically and experimentally in regular sea. Looking at Fig. 13 and Fig. 14, an almost triangular instability region with the presence of a minimum threshold can be guessed. The behaviour, thus, recall the instability regions reported in Fig. 3.

The problem of deciding whether or not a case has to be considered as stable or not from the analysis of only one realization of the process is clearly represented by Fig. 15. In this figure two different realization of the same process have been reported. In the first case (upper time

history), after the initial perturbation, the roll motion time history clearly shows the presence of a solution above the stability threshold.

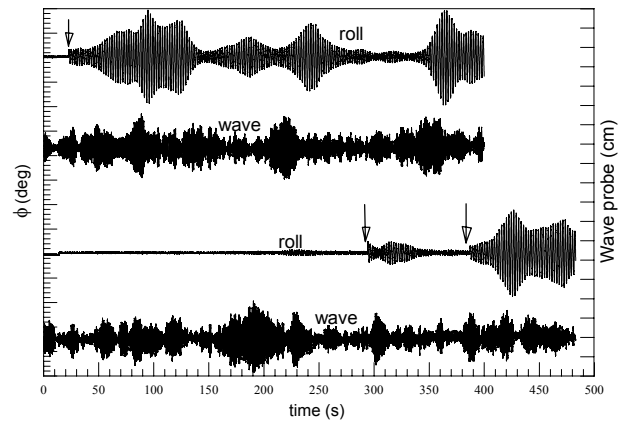


Fig. 15: Two different realizations of the phenomenon of parametric rolling with the same sea spectrum (NB,  $V = 0.3\text{ m/s}$ ,  $H_{1/3}/L_{BP} = 1/132$ ). Arrows indicate external perturbations.

In the lower graph, before the first perturbation the motion seems to be stable, and after the first perturbation roll seems to decay. Such a case would have been catalogued as a stable condition, if a second perturbation had not been applied. After the second perturbation, a behaviour typical for conditions inside the instability region can be seen. The experimental evaluation of the threshold is, thus, likely to be associated to a quite large level of uncertainty.

The last question needing an answer is:

*“Does a threshold exist below which the motion can be considered as stable?”*

The answer to this question is implicit in the answer to the previous problem. From Fig. 13 and Fig. 14, the presence of a threshold as a function of the speed is clearly shown. The dependence of the value of the threshold from the type of spectrum can be clearly seen in Fig. 16.

Some qualitative considerations can be done:

- a threshold exists beyond which the solution  $\phi = 0$  is unstable
- the narrower the spectrum, the lower the threshold
- the narrower the spectrum, the larger the standard deviation of the roll motion, given the significant wave height

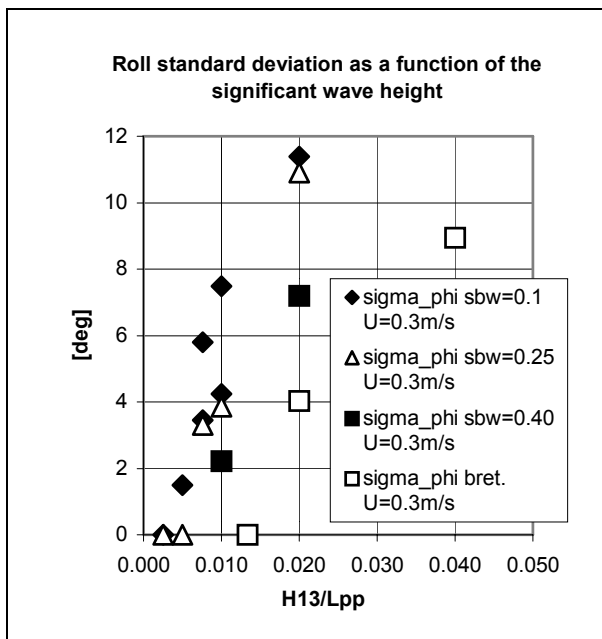


Fig. 16: Relation between significant wave height, roll standard deviation and spectrum type in the case of model speed equal to 0.3m/s.

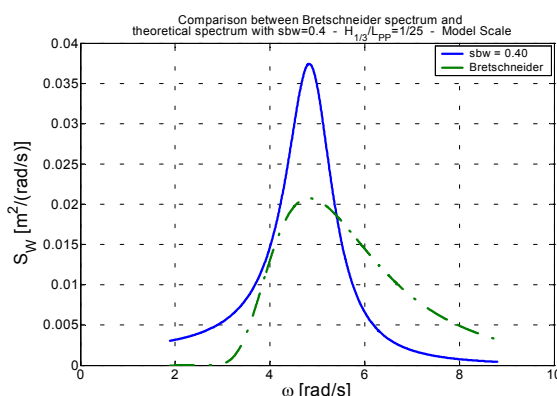


Fig. 17: Comparison between Bretschneider spectrum ( $sbw = 0.425$ , dash-dotted line) and LB spectrum ( $sbw = 0.400$ , solid line). Model scale.

It's extremely interesting to compare the results obtained for the Bretschneider spectrum and the spectrum named "LB", that is the theoretical spectrum with  $sbw = 0.4$ . The two spectra are reported in Fig. 17 for a significant wave height of 5.3m at full scale.

Although the significant wave height is the same for both spectra, the way the energy is distributed in the frequency domain is completely different. The LB spectrum shows a large part of energy at low frequency (long waves), whereas the conversely occurs for the Bretschneider spectrum, that has a large part of energy at frequencies higher than the modal frequency (short waves).

Moreover the percentage of energy in the vicinity of the modal frequency is larger for the LB spectrum than for the Bretschneider. Short waves are less effective in promoting the build up of parametric rolling, due to the small value of the ratio between wavelength and ship length [3],[6].

The aforementioned differences between the two spectra explain the behaviour of the curves in Fig. 16.

### 3.3 Mathematical modelling

#### Prediction of stability boundary and behaviour above threshold in the stochastic case – Introduction

In order to try to analyse the phenomenon of parametric rolling in a stochastic environment, two approaches have been used, based on the works of Rong et al. [18] and Roberts [16]. The analytical results from Roberts have already been used in the past by Skomedal [19] to assess stability boundaries related to parametric excitation in beam and following sea.

In the work of Rong the method of multiple scales is used and the solution to the stochastic

problem is obtained as a perturbation of the deterministic solution. Damping is supposed to be linear. Nonlinearities of the restoring moment are taken into account with a constant cubic coefficient. This approach has been used in order to try to predict both the threshold (that depends on the linear part of the motion equation) and the amplitude of motion above threshold (because the major cause of boundness is the detuning effect).

In the work of Roberts, based on the stochastic averaging technique, the nonlinearities of the righting arm and those related to the damping term are decoupled. Thus the amplitude above threshold is bounded only by the nonlinear effects of damping. From experiments, analytical results and simulation, it has been shown that, when parametric excitation is large, the principal factor determining the extent of the instability region and the amplitude of motion above threshold are the nonlinearities of the restoring moment (although nonlinear damping has an interesting role in avoiding the erosion of the safe basin and in limiting very large motion spikes). The damping term alone can't be used for predicting amplitude of motion above threshold, thus the analytical results obtained by Roberts have been used only in order to predict the stability boundary.

### The modelling of metacentric height fluctuation

In the following analysis the modelling of the metacentric height fluctuation as a stochastic process will be needed. In order to model the metacentric height spectrum, a linear approach based on the work of Dunwoody [3] has been used.

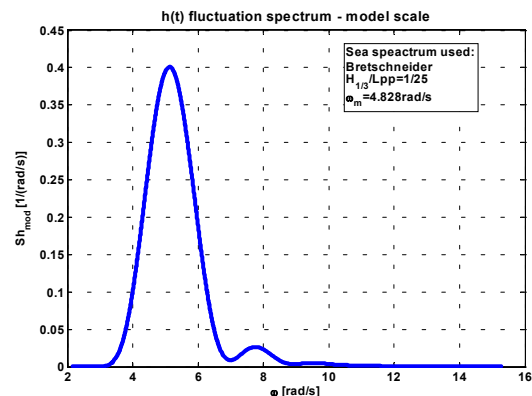


Fig. 18: Example of predicted spectrum for the nondimensional metacentric height fluctuation  $h(t)$ . Bretschneider sea spectrum.

The transfer function of the fluctuation of  $\overline{GM}$  has been estimated using the analytical formula given in [3], thus from the given sea spectrum, the spectrum of the relative fluctuation of the metacentric height  $h(t)$  has been obtained. In this approach the ship is seen as a linear filter between the sea elevation and the metacentric height fluctuation. The quasi-static assumption and the hypothesis of slender ship are done in [3]. A typical spectrum of  $h(t)$  is shown in Fig. 18. The characteristic multi-modal behaviour is due to the particular shape of the transfer function for  $h(t)$ , that shows many oscillations when the wave length is shorter than the ship length [2], [3], [8].

### Stability boundaries – Fokker-Planck method [16]

The motion is described by the following equation

$$\ddot{\phi} + 2\nu \cdot \omega_0 \cdot \dot{\phi} + d_{nl}(\dot{\phi}) + \omega_0^2 \cdot (1 + h(t)) \cdot \phi + \alpha_3 \cdot \phi^3 = 0 \quad (14)$$

being  $d_{nl}(\dot{\phi})$  the nonlinear damping component.  $h(t)$  is supposed to be a gaussian stationary process with zero mean and spectrum (single side)  $S_h(\omega)$ . The equation is analysed in [16] by means of the stochastic averaging technique

and Fokker-Planck equation. Stability condition is given on the base of the existence of a nontrivial stationary probability density function for the process (sample stability) and for the n-th statistical moments (stability of the n-th moment). The condition for sample stability is given by

$$\nu > \frac{\pi}{8} \cdot \omega_0 \cdot S_h(2\omega_0) \quad (15)$$

In order to obtain  $S_h(2\omega_0)$ , the spectrum of  $h(t)$  is estimated at zero speed and then Doppler effect is applied to obtain the spectrum of the fluctuation at the encounter frequencies.

The value of significant wave height  $H_{1/3,lim}$ , at each speed, for which the following condition is satisfied

$$\nu = \frac{\pi}{8} \cdot \omega_0 \cdot S_h(\omega_e = 2\omega_0, V, H_{1/3,lim}) \quad (16)$$

gives the stability threshold in the  $(V, H_{1/3} / Lpp)$  plane.

#### Stability boundaries – Multiscale method [18]

The motion equation is supposed to be of the following form:

$$\ddot{\phi} + 2\nu \cdot \omega_0 \cdot \dot{\phi} + \omega_0^2 \cdot (1 + h(t)) \cdot \phi + \alpha_3 \cdot \phi^3 = 0 \quad (17)$$

$h(t)$  is supposed to be a narrow band, stationary gaussian process with zero mean. Thus  $h(t)$  can be expressed by means of two slowly varying functions (phase  $\gamma(t)$  and envelope  $m(t)$ ) in the following form [14],[18]

$$h(t) = m(t) \cdot \sin(\Omega_1 \cdot t + \gamma(t)) \quad (18)$$

$m(t)$  is Rayleigh distributed, whereas  $\gamma(t)$  has a uniform distribution in  $[0, 2\pi]$ . Following Panjaitan [14],  $\Omega_1$  is the mean frequency defined as

$$\Omega_1 = \frac{\int_0^{+\infty} \omega_e \cdot S_h(\omega_e) d\omega_e}{\int_0^{+\infty} S_h(\omega_e) d\omega_e} \quad (19)$$

The solution of equation (17) is supposed to be of the form

$$\phi(t) = 2 \cdot a(t) \cdot \cos\left(\frac{\Omega_1}{2} \cdot t - \frac{\Theta(t) - \gamma(t)}{2}\right) \quad (20)$$

The unknown functions  $a(t)$  and  $\Theta(t)$  are split in their mean value and fluctuation as follow:

$$\begin{cases} a(t) = a_0 + a_1(t) \\ \Theta(t) = \vartheta_0 + \Theta_1(t) \end{cases} \quad (21)$$

$m(t)$  is supposed to show little fluctuations around its mean value, that is

$$\begin{cases} m(t) = E\{m\} + \delta m(t) \\ \delta m(t) \ll E\{m\} \\ E\{m\} = \sqrt{\frac{\pi}{2}} \cdot \sigma_h \end{cases} \quad (22)$$

being  $\sigma_h$  the standard deviation of the process  $h(t)$ . The expected value of the envelope

$$E\{C(t)\} = 2 \cdot E\{a(t)\} = 2a_0 \quad (23)$$

can be obtained from

$$\begin{cases} E\{C(t)\} = \sqrt{\frac{4\omega_0}{3 \cdot \alpha_3}} \cdot \sqrt{s \pm \frac{\omega_0}{2} \cdot \sqrt{E^2\{m\} - (4 \cdot \nu)^2}} \\ s = \Omega_1 - 2 \cdot \omega_0 \end{cases} \quad (24)$$

The minimum threshold can be calculated as

$$E\{m\} = 4 \cdot \nu \quad (25)$$

The same boundary has been found by Dunwoody [4] as a sample stability limit.

From the limiting standard deviation for the process  $h(t)$ , the corresponding limiting significant wave height can be evaluated.

It is worth recalling that the variance of the process  $h(t)$  is supposed to be not dependent on the speed. The minimum threshold will be reported in the following graphs as a horizontal line in the plane  $(V, H_{1/3} / L_{pp})$ . Moreover, the position of the two bifurcation points can be obtained for each significant wave height. Under the conservative assumption of zero damping (far from the speed of perfect synchronism  $s = 0$ , the influence of damping is negligible when large parametric excitations are considered), from equation (24), one obtains:

$$s_{1,2} = \pm \frac{\omega_0}{2} \cdot E\{m\} = \pm \frac{\omega_0}{2} \cdot \sqrt{\frac{\pi}{2}} \cdot \sigma_h(H_{1/3}) \quad (26)$$

Using the expressions governing the Doppler effect, the speeds leading to the corresponding values for  $\Omega_1$ , can be obtained.

It's important to note that the bifurcation points coincides, as a first order approximation, with the points obtained by the intersection of an horizontal line (at the given value of  $E\{m\}$ ) with the boundaries of the instability region in the deterministic stability chart (Fig. 3). Thus the minimum threshold value and the couple of lines giving the position of bifurcation points are a first approximation of the instability region.

### 3.4 Comparison between experimental and theoretical stability threshold

The stability charts for the cases of narrow band ( $sbw = 0.1$ ) and Bretschneider sea spectra are reported in

Fig. 19 and

Fig. 20 respectively. These two spectra are the narrowest and the largest regarding the value of the spectral bandwidth. The stability boundaries obtained by using the multiscale method and by using the Fokker-Planck method are marked MS and FP respectively. Dashed curves in Fig. 20 correspond to stability limits obtained by taking into consideration the saturation effect of the transfer function of the metacentric height fluctuation, as reported in [8]. The presence of two minima in the stability limit curve obtained by means of the Roberts' approach depends on the multi-modal nature of the spectrum of  $h(t)$ . The experimental stability conditions are reported as follows:

- black squares: unstable
- white squares: uncertain
- white diamonds: stable
- 

First of all it can be said that the behaviour of the stability boundaries is reproduced by the analytical results. In both cases there are no unstable conditions outside the boundaries, for both approaches. The proposed procedure can thus be considered "on the safe side". First of all it can be said that the behaviour of the stability boundaries is reproduced by the analytical results. In both cases there are no unstable conditions outside the boundaries, for both approaches. The proposed procedure can thus be considered "on the safe side".

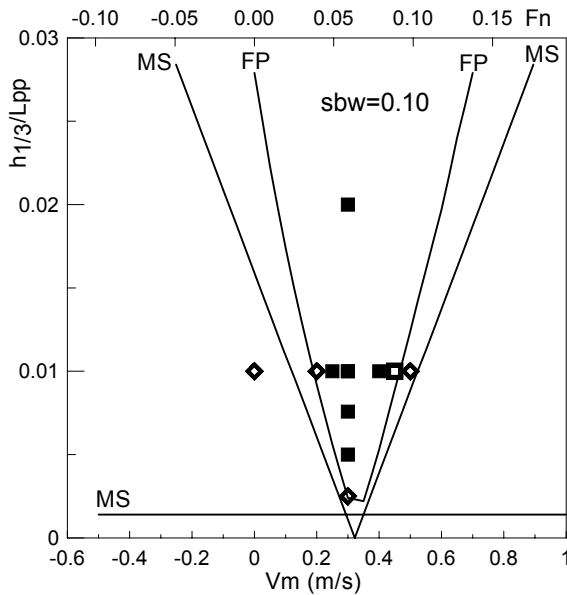


Fig. 19: Stability boundaries for the narrow band (NB) sea spectrum.

In the case of narrow band spectrum ( Fig. 19) a very good agreement is found between limits evaluated using Roberts' approach and experimental results. In the same case the approach of Rong overestimates the width of the instability region. The minimum threshold evaluated with the multiscale method is smaller than the threshold calculated with the Fokker-Planck method, and the latter better represents the experimental behaviour.

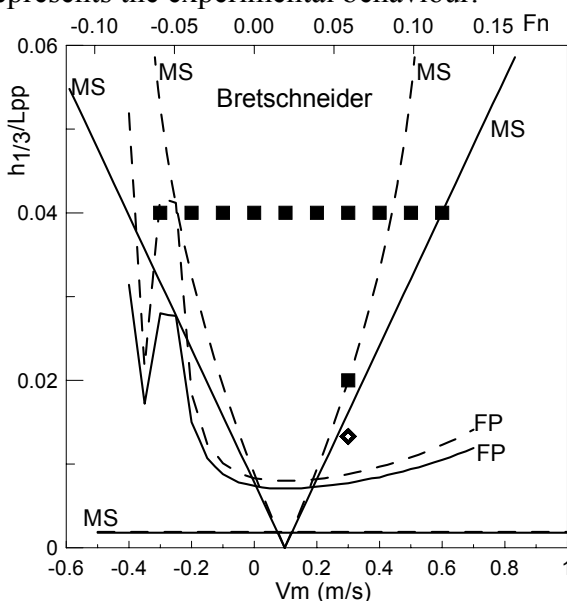


Fig. 20: Stability boundaries for the Bretschneider sea spectrum.

In the case of Bretschneider spectrum ( Fig. 20), only one point flagged as stable is available. Is thus difficult to draw ultimate conclusions about the minimum threshold. Regarding the width of the instability zone, the approach of Rong seems to give a good agreement with experimental results, while Roberts' approach cannot be discussed in detail. Using the semi-empirical correction for nonlinear relation between wave height and amplitude of metacenter fluctuation gives even a worst agreement with experiments in both cases.

The use of bifurcation points as stability limits, although not theoretically correct, seems to be a quite good tool. The idea of using the position of bifurcation in order to draw a stability boundary arose by the experimental evidence that, outside a certain range of speed, in regular sea, no resonant solutions have been found. The same seems to hold in a somewhat similar way for the stochastic case (Fig. 12).

### 3.5 Comparison between predicted and estimated statistical averages above threshold

The following quantities have been estimated for each experiment:

- mean value of the roll envelope  $A_{medio}$
- significant roll amplitude  $A_{1/3}$
- maximum roll angle  $A_{max}$

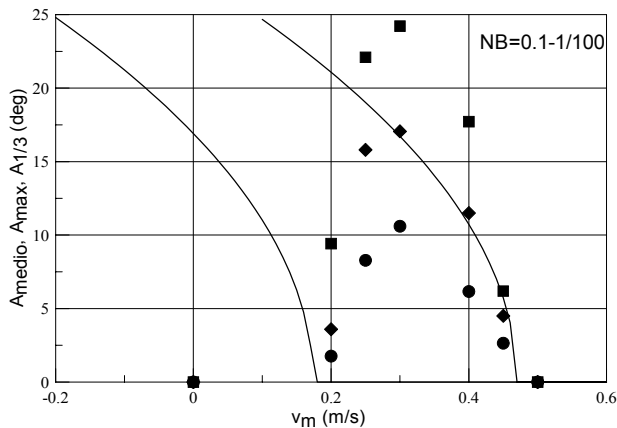


Fig. 21: Comparison between experimental results and predicted mean amplitude. NB spectrum.

The obtained values have been compared with the predicted *expected* value of the roll envelope using equation (23). The cubic restoring coefficient has been estimated from the still water righting arm. The results are reported in Fig. 21 and Fig. 22. In the figures  $A_{medio}$  is reported as circles,  $A_{1/3}$  as diamonds and  $A_{max}$  as squares.

The agreement between predicted mean amplitude and estimated mean amplitude from experiments is completely unsatisfactory. Prediction largely overestimates the experimental results. A good agreement can be seen, instead, between the analytical curves and the values of  $A_{1/3}$ .

A rigorous explanation for this fact has not been found; but, from a qualitatively point of view, it seems that the prediction is able to represent somewhat that can be referred as “the mean value of the *activated* process”. Calculating the mean only on the 1/3 of the highest roll amplitudes coincides with filtering the part of motion associated with small amplitudes, where the achieving of a stationary condition above threshold is doubtful. The phenomenon of parametric rolling in irregular longitudinal sea is known to be a phenomenon that has to be “switched on” ([19], Fig. 15) and that can stay “switched off” for long periods.

This fact introduces some problems in the statistical analysis of the time histories.

This problem needs further attention and should be tackled both experimentally and, maybe firstly, numerically (by means of Monte Carlo simulation, for example).

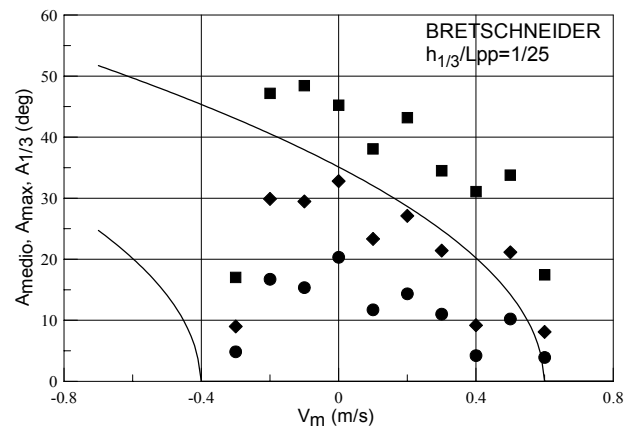


Fig. 22: Comparison between experimental results and predicted mean amplitude. Bretschneider spectrum.

### 3.6 Future work

The obtained predictions for the stability boundaries have shown to be in very good qualitative agreement with the experimental results. The approximation of narrow band process for the metacentric height fluctuation seems to give a quite good quantitative agreement when the sea spectrum is extremely narrow. Unfortunately the results are quantitatively worst when the spectral bandwidth of the sea spectrum is larger.

Regarding the prediction of the statistical averages above threshold, the proposed approach overestimates the quantity it should predict, that is the average of the roll envelope amplitude, but the width of the instability zones seems to be quite well reproduced. Because of the fact that, in the used model, the amplitude above threshold depends linearly on the inverse of the square root of the cubic restoring coefficient (see equation (24)), whereas the



width of the instability region depends almost only on the standard deviation of the parametric excitation, it can be said that, probably, a better modelling of the nonlinear restoring is needed, whereas the level of parametric excitation have been quite well modelled. The cubic restoring coefficient has been shown to be, actually, time dependent, both in regular sea (equation (8)) and in irregular sea [8]. A correct modelling of the correlation, in irregular sea, between the fluctuation of linear and nonlinear term would hopefully lead to a reduction of the statistical averages above threshold, and, thus, a to better agreement with experiments.

Moreover, the problem of a correct analysis of the experimental data should be solved: which parts of the experimental record should be used in order to obtain the statistical averages? The complete record, or only the part showing, clearly, the presence of parametric rolling? And what does “clearly” mean from a mathematical point of view?

Regarding the bandwidth of the process, the analytical results shown in this paper have been obtained by the respective authors (Roberts and Rong) by means of the approximation of narrow band process for the metacentric height fluctuation. In the work of Rong et al. [18] a numerical validation of the analytical results has been performed using a very narrow spectrum. The same has not been done in the case of the work of Roberts [16]. It would be interesting to understand whether or not the analytical results obtained in such an approximation can be used for not narrow spectra (although the border between large band and narrow band process is not, and can't be, sharp). A numerical investigation by means of Monte Carlo simulations, using somewhat like a “standard” spectrum for the process  $h(t)$  would be very useful. Moreover, if only the stability boundaries are of concern, a completely linear model can probably be used.

## 4 CONCLUSIONS

In this paper the experimental results for the parametric rolling of RoRo ship in regular and irregular longitudinal waves have been reported. A mathematical modelling of the 1.5-DOF roll motion has been proposed in the case of both regular and irregular sea. In the case of regular sea a good agreement between experimental results and prediction have been obtained, both with a fully analytical and a fully numerical approach. Some problems must be solved regarding the modelling of the restoring lever fluctuation in regular waves. Taking into consideration the vertical motions in waves will certainly lead to a better prediction of the experimental results, but this will make the modelling more complicated. If the target of the study is a simple model able to give good, but not necessary very exact prediction of the roll response above threshold, too many complications should be avoided, especially if one wants to use an analytical approach in order to give the roll response curve in a quite closed form.

From the reported results, it seems that a model using the fluctuation of the  $\overline{GZ}$  curve evaluated by a fix trim hydrostatic approach can be considered “on the safe side”, and can well predict the maximum roll amplitude inside the instability region. Some problems have been encountered for the smallest tested waves.

Regarding the comparison between experimental results and analytical prediction, it seems that the proposed model is able to give a prediction of the stability boundaries “on the safe side” too. Unfortunately the predicted minimum threshold seems to be too conservative. The minimum threshold not only depends on the level of linear damping and on the relation between significant wave height and metacentric height standard deviation, but depends on the particular definition of stability one wants to use (sample stability, stability of the mean, stability of the mean square,...). The



limiting significant wave height could differ from that calculated using the sample stability definition, even by 50% or 100%, depending on the used formula. Thus an agreement on a "standard" practical definition of stochastic stability should be found.

Regarding the behaviour of the statistical averages above threshold, a very good qualitative agreement has been found in spite of the simplicity of the used model. Concerning the quantitative predictions, some problems arose that need further numerical and experimental research.

## 5 ACKNOWLEDGMENTS

This research has been developed with the financial support of INSEAN under contracts "Study of the Roll Motion in Longitudinal Waves" and "Study of the Roll Motion in Longitudinal Irregular Waves" in the frame of INSEAN Research Plan 2000-2002. During the redaction of this paper Prof. Francescutto has been guest of Hiroshima University, Faculty of International Development and Cooperation, in the frame of a Visiting Professorship scheme.

## 6 REFERENCES

- [1] Bogdanov, P., Dimitrova, S., Kishev, R., "On The Influence of Restoring Moment Changes in Waves on Stability Estimations", Proc. 4<sup>th</sup> STAB Intl. Conference, Napoli, pp. 409-415, 1994.
- [2] Bulian, G., "Rollio parametrico in mare regolare e stocastico", Graduation Thesis, University of Trieste, October 2002.
- [3] Dunwoody, A. B., "Roll of a Ship in Astern Seas – Metacentric Height Spectra", J. Ship Research, Vol. 33, pp. 221-228, 1989.
- [4] Dunwoody, A. B., "Roll of a Ship in Astern Seas – Response to GM Fluctuations", J. Ship Research, Vol. 33, pp. 284-290, 1989.
- [5] Francescutto, A., "Stochastic Modelling of Nonlinear Motions in the Presence of Narrow Band Excitation", Proc. Int. Symp. ISOPE'92, San Francisco, Vol. 3, pp. 554-558, 1992.
- [6] Francescutto, A., "Theoretical Study of the Roll Motion in Longitudinal Waves", Technical Report, (in Italian), Dept. DINMA, University of Trieste, 2002.
- [7] Francescutto, A., Bulian, G., "Nonlinear and Stochastic Aspects of Parametric Rolling Modelling", Proc. 6<sup>th</sup> Int. Workshop on Ship Stability, Webb Institute, New York, October 2002.
- [8] Francescutto, A., Bulian, G., "Theoretical and Experimental Study of Roll Motion in Longitudinal Irregular Waves", Technical Report, (in Italian), Dept. DINMA, University of Trieste, 2003.
- [9] Francescutto, A., Dessi, D., Penna, R., "Some Remarks on the Nonlinear Modelling of Parametric Rolling", Proc. 11<sup>th</sup> Int. Symp. ISOPE'2001, Stavanger, Vol. 3, pp. 317-320, 2001.
- [10] Goda, Y., "Random Seas and Design of Maritime Structures", University of Tokyo Press, 1985.
- [11] Hayashi, C., "Nonlinear Oscillations in Physical Systems", New York, McGraw Hill, 1964.
- [12] Ibrahim, R. A., "Parametric Random Vibration", Research Studies Press, Wiley, New York, 1985.

- 
- [13] Odabashi, A. Y., "Stochastic Stability of Ships in Following Seas", Proc. 1<sup>st</sup> Int. Conf. IMAEM, Istanbul, pp. 603-617, 1978.
- [14] Panjaitan, J. P., "A Study on Ship Motions and Capsizing in Severe Astern Seas", Ph.D. Thesis, Dept. NAOE, Osaka University, 1998.
- [15] Paulling, J. R., "The Transverse Stability of a Ship in a Longitudinal Seaway", J. Ship Research, Vol. 4. , pp.37-49, 1961.
- [16] Price, G. W., "A Stability Analysis of the Roll Motion of a Ship in an Irregular Seaway", Int. Shipb. Progress, Vol. 22, pp. 103-112, 1975.
- [17] Roberts, J. B., "Effect of Parametric Excitation on Ship Rolling Motion in Random Waves", J. Ship Research, Vol. 26, pp. 246-253, 1982,.
- [18] Rong, H., Xu, W., Fang, T., "Principal Response of Duffing Oscillator to Combined Deterministic and Narrow-Band Random Parametric Excitation", J. Sound and Vibration, Vol. 210(4) , pp. 483-515, 1998.
- [19] Skomedal, N. G., "Parametric Excitation of Roll Motion and Its Influence on Stability", 2<sup>nd</sup> STAB Intl. Conference, Tokyo, pp. 113-125, 1982.
- [20] Spyrou, K.J., "Designing Against Parametric Instability in Following Seas", Ocean Engng 27, pp. 625-653, 2000.

